Design Optimization and Probabilistic Assessment of a Vented Airbag Landing System for the ExoMars Space Mission

Richard Slade, Andrew Kiley
EADS Astrium Ltd
Stevenage, SG1 2AS, UK
richard.slade@astrium.eads.net, andy.kiley@astrium.eads.net

Vassili Toropov
University of Leeds
Leeds, West Yorkshire, LS2 9JT, UK
v.v.toropov@leeds.ac.uk

First published in 2007

Abstract

Vented airbag systems offer an attractive means of cushioning the landing impact of robotic planetary spacecraft. This type of airbag absorbs the impact kinetic energy by exhausting the inflation gas through vent patches in a controlled way that aims to bring the lander to rest with minimum rebound, limited deceleration and in an upright attitude. Such systems are characterised by highly non-linear behaviour. This, coupled with the difficulty of adequate terrestrial testing results in an analytical approach to design that relies on explicit finite element (FE) analysis. However, the simulation of an impact of a few tenths of a second duration typically requires tens of hours of CPU time, making it impractical to optimise a design using a trial end error approach and to perform the large number of analysis runs necessary for a probabilistic assessment of varied landing conditions. This paper presents a methodology for overcoming these problems with reference to a vented airbag design for the ESA ExoMars mission. The approach utilises the Moving Least Squares Method (MLSM) to fit high quality approximations to multi-dimensional response surfaces from a relatively small number of FE analysis runs. This method is well-adapted to highly non-linear and 'noisy' response surfaces that are typical for this problem. The surrogate response surfaces were used to locate an optimum in the 'design parameter space' and to perform 10,000 sample point Monte Carlo runs in a probabilistic assessment of reliability due to varying landing conditions.

Keywords: HyperStudy, ExoMars, Moving Least Squares, LsDyna

1.0 Introduction

The landing of robotic spacecraft on Mars is a risky undertaking. Approximately half of all attempts have failed. Several approaches to the landing problem are possible, ranging from autonomous fully-guided rocket-braked soft-landing systems to more passive concepts using parachutes and airbags to provide a semi-hard landing. The latter are particularly attractive for lower cost, lower mass missions.

1.1 Un-vented Airbags

Airbags have been employed on space probes from the Russian un-manned moon missions of the 1960s through to the more recent Mars Pathfinder (MPF), Mars Explorer Rover (MER) and Beagle2 missions. These all employed the un-vented, or "bouncy ball", type of airbag **(Figure 1)**. The principle consists of completely surrounding the payload with a protective cocoon of airbags which are compressed during the landing impact. Since the gas is not vented, there is little energy dissipation and the impact kinetic energy is almost all returned, resulting in typically twenty or more bounces before coming to rest. To provide all-round protection and abrasion resistance results in heavy airbags and also requires a substantial lander structure with a self-righting capability.

Figure 1: Un-Vented ("bouncy ball") Airbags. Left: Mars Pathfinder [NASA/JPL]. Right: Beagle 2, After Lander Release [Beagle2]

1.2 Vented Airbags

Because mass is such a precious commodity in any Mars mission, an alternative vented airbag concept has been proposed for low cost robotic landers that can offer a significant reduction in mass and therefore increased useful lander payload capacity[1].The essential feature of the vented airbag concept is that the gas is exhausted to the atmosphere during impact to provide a means of dissipating the impact kinetic energy. In an ideal design, the lander comes to rest in a single stroke with no rebound, hence this type of airbag is also termed “dead-beat”. Since multiple bounces are eliminated, it is only necessary to protect the underside of the lander (with a less abrasion-resistant material) which reduces the airbag fabric mass. Further mass savings are possible in the gas storage or generation system and the lander structure, which can be reduced to a simple platform **(Figure 3)**.

Vented airbags have not been employed on any planetary landers to date, but the concept has a long heritage in a number of terrestrial applications such as low level supply dropping from aircraft, and the recovery of remotely piloted vehicles, rocket boosters and military aircraft crew escape capsules. The application to robotic Mars landers brings some unique problems related to the effects of a low atmospheric pressure (mainly CO_2 at about 0.5% of Earth sea-level pressure) and low gravity (38% of Earth). Testing on Earth can never fully reproduce the true landing conditions and this therefore puts an emphasis on accurate analytical modeling, correlated by only a limited number of tests.

Actuation of the vents introduces an active control element not present with the un-vented airbag type. Several control approaches are possible, ranging from simple burst patches through to more complex strategies employing pyrotechnically-actuated vents triggered by algorithms running on the on-board computer that take data from sensors such as accelerometers, laser range-finders, close proximity radar or cameras. These systems can be reactive, i.e. adopt a vent strategy that reacts to the sensed behaviour during impact, or predictive, i.e. determine a vent strategy based on sensed conditions prevailing immediately prior to impact. With impact event durations of less than 100ms, the former approach requires fast sensor sampling and simple algorithms to give the necessary reaction times. Experience suggests that the simplest, self-actuated burst pressure patch is unreliable and doesn’t provide sufficient control. The separation of sensors and actuators is therefore the preferred approach, either in reactive or predictive control systems[2].

One of the biggest challenges in the design of a vented airbag system is stabilising the attitude during the landing to prevent roll-over whilst at the same time preventing excessive rebound. The tendency to roll over is caused primarily by the lateral component of velocity (ground speed) and is exacerbated by pitch attitude and pitching angular velocities. For descent under a parachute, the lateral velocity component is that of the local prevailing wind at the height of the canopy. Stabilising the attitude during impact can be achieved with a low centre of mass and multiple separate airbags with a large spatial separation to provide reaction moments. For compact Mars landers (necessitated by the need for encapsulation within a protective aeroshell for atmospheric entry) this is not generally possible, in which case the alternative approach is to divide a single envelope into multiple compartments, each with an independently controlled vent.

2.0 ExoMars Vented Airbag Concept

ExoMars is the European Space Agency’s first flagship mission in its Aurora exploration program of the solar system. Its objective is to land a rover on Mars with an exobiology payload to search for signs of extinct or existing microbial life **(**Error! Reference source not found.**)**. The 240kg rover is equipped with a drill for acquiring samples from two metres below the harsh environment at the surface and an on-board analytical laboratory containing a total of 21 scientific instruments plus sample acquisition, preparation and handling systems.

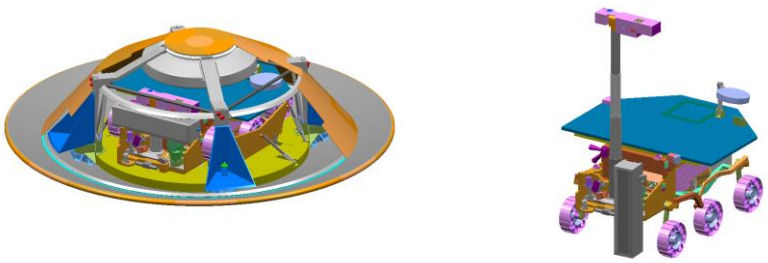

Figure 2: ExoMars. Top: Rover Encapsulated within Descent Module for Atmospheric Entry. Bottom: Deployed Rover During Drilling [ESA]

The ambitious payload mass fraction requires a highly efficient Entry, Descent and Landing System (EDLS). A rocket controlled soft landing has been discounted largely on the grounds of development cost and schedule, leaving a choice between un-vented and vented airbag systems, both employing large parachutes to limit descent velocity, possibly augmented with solid retro-rockets. The un-vented ("bouncy ball") type offers a flight-proven heritage at higher mass, whereas the vented ("dead-beat") type has the potential to reduce mass, but represents an untried concept in this application with an unknown performance. The vented design is perceived as being more susceptible to high wind speeds but more robust in rocky terrain since it has a better tolerance to fabric rupture (fabric tears have the effect of increasing what are already large vent areas, whereas a ruptured "bouncy ball" will deflate, providing no protection for subsequent impacts).

The baseline ExoMars vented airbag design adopted for the study is shown in **Figure 3**. The stowed rover is mounted on the upper surface of a stiff circular platform below which the airbag is inflated during parachute descent. The main airbag envelope is divided into 6 compartments by impermeable radial diaphragms and each compartment has a large vent patch to the outside atmosphere on its upper surface. The vent patches consist of segmented circular areas of fabric with an internal lightweight impermeable liner. The fabric segments are held by a cord that passes through a pyrotechnic cutter. Cutting the cord causes the liner to rupture and open the fabric segments like petals allowing the gas to be exhausted through the resulting orifice.

Inside the main airbag envelope is an inner toroidal bag, located directly under the platform running around its circumference, inflated to a higher pressure than the other compartments. This "anti-bottoming" bag is not vented during the impact but provides a final landing cushion to absorb the residual kinetic energy.

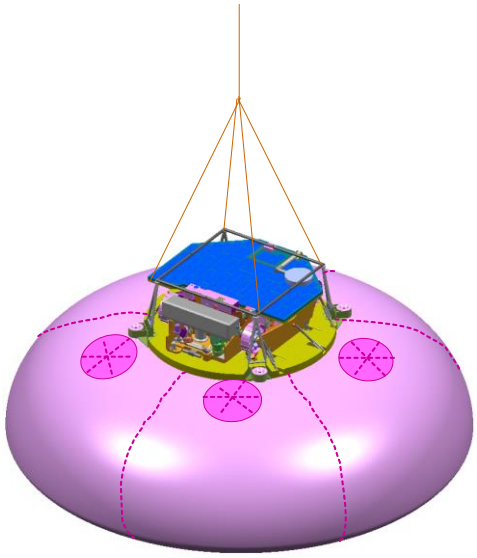

Figure 3: Baseline ExoMars Vented Airbag Concept

For the study, the airbag venting control was limited to a simple reactive system in which all 6 compartments were vented simultaneously once an acceleration threshold of 65g (resultant measured at the payload centre of mass) was exceeded. The compartmented design permits more sophisticated differential venting strategies, but the initial objective was to explore the performance envelope of this scheme before increasing the system complexity.

The vertical velocity at impact was fixed at 25 m/s, as determined by the lander terminal velocity under the parachute at the landing site altitude. This relatively high speed reflects the low density of the Martian atmosphere, particularly at the high altitude landing sites considered for ExoMars (up to 2 km above the Mars datum). The 25 m/s landing velocity was determined from a separate EDLS level optimization study in which the combined mass of the parachute and airbag system was minimised using simple parametric sizing models. This velocity is a compromise between a large parachute canopy necessary for a low landing speed and a large airbag necessary for a high landing speed.

3.0 Study Objectives

The objectives of the study were to develop methods for the design optimization and robustness analysis of vented airbags. In particular, to support the design of the ExoMars mission, the following key questions were posed:

1) What is the geometry and mass of an optimised vented airbag system?
   - to permit a trade-off comparison with the un-vented type.

2) What is the probability of a successful landing?
   - to assess the robustness of the design and quantify its reliability.

3) What is the sensitivity of the landing success probability to changing landing scenarios?
   - to quantify the effect on reliability of changes in landing site, parachute performance etc.

The remainder of this paper describes how these questions were addressed using FE analysis and surrogate response modelling techniques.

4.0 Analysis Overview

The non-linear effects of large airbag deformation, varying contact conditions, gas compressibility and gas discharge means that transient explicit finite element analysis is the only viable means of accurately modelling impact behaviour. The primary impact event durations are typically up to about 100ms, although longer analysis durations are necessary in cases where there is significant rebound or multiple contacts. The resulting simulation times are of the order of 10 hours, making an iterative design optimization computationally expensive and a probabilistic robustness assessment requiring 100s or 1000s of Monte Carlo simulations impractical.

To overcome these problems, a response surface approximation or surrogate modelling approach was adopted. A response surface gives the value of a key output variable in the design space, e.g. peak deceleration or airbag fabric stress, as a function of design variables such as airbag diameter, inflation pressure, vent area etc. N input variables yield N-dimensional response surfaces. The number of FE analysis runs to fully calculate the response surfaces quickly becomes unmanageable, even with only a handful of design variables. In the surrogate modelling approach, the response surfaces are approximated from a relatively small number of FE analysis runs by using advanced surface-fitting algorithms. Once generated, the set of approximated response surfaces provide a surrogate model which can be used to solve the constrained optimization problem with minimal computational effort. The same method can be used to perform a probabilistic assessment. Here, the surrogate response model is developed in terms of landing variables, such as wind speed, rock size etc, and is then used in conjunction with probability models of the variables in a Monte Carlo analysis. Thousands of simulations of the surrogate model can be run in a few minutes.

The overall analysis methodology is summarised in Error! Reference source not found.. The core analysis process is the same for both the design optimization and the probabilistic robustness/reliability assessment. The basic steps consist of: defining the design (or landing condition) variables; selecting the combinations of variables for FE analysis using a Design of Experiments (DoE) method; performing the FE analyses for these cases; fitting surrogate response surfaces through the output data using a surface-fitting algorithm and finally using these either to solve the optimization problem or to perform Monte Carlo simulations. The management of the complete process was performed using HyperStudy software **[3]**.

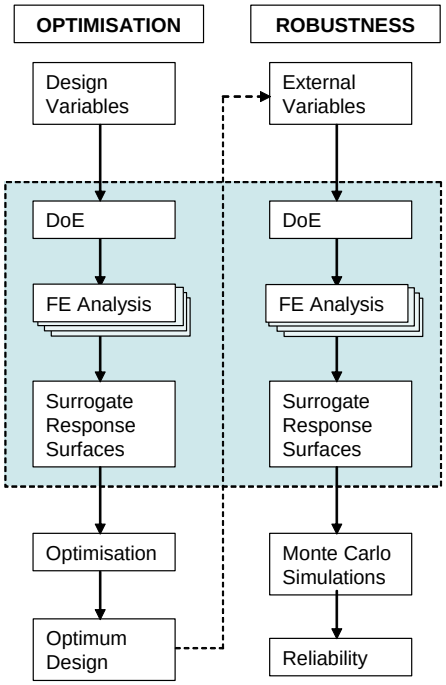

Figure 4: The Analysis Process for Design Optimization (left) and Robustness Assessment (right), using the same Response Surface Approximation Technique

5.0 Finite Element Model Analysis

The explicit FE analysis was performed using LS-DYNA **[4]**. The geometry and mesh of the baseline model is shown in **Figure 4**. Model parameters are summarised in **Table 1**.

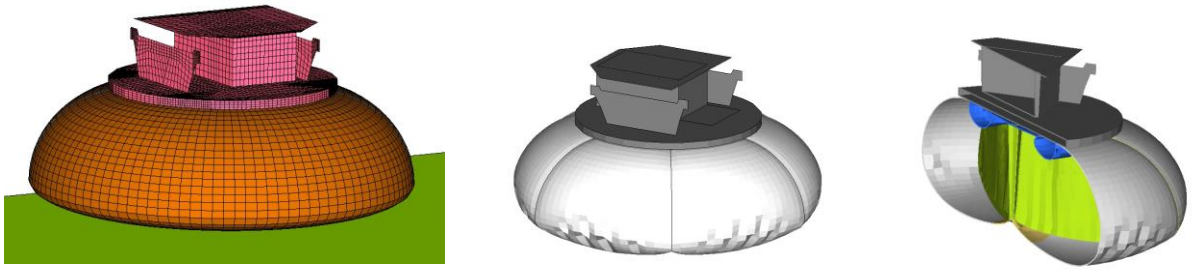

Figure 4: Baseline FE Model. Left: Un-inflated Geometry and Mesh. Centre: Inflated Geometry. Right: Cross-section Showing Internal Diaphragms (green) and Anti-Bottoming Toroid (blue)

The stowed rover and platform were modelled as rigid elements with the appropriate mass and inertia properties. The airbag envelope was idealised as a membrane with linearly elastic isotropic stiffness, but with the shear modulus set to a very low value (consistent with numerical conditioning) to represent the behaviour of the woven fabric.

The analysis simulation covered 3 stages: airbag inflation, initial impact and venting. To permit batch processing, it was necessary to minimise the solution times and automate the analysis stages so they could be run sequentially

without user intervention. For the inflation step, the dynamic relaxation feature within LS-DYNA was utilised to avoid the long solution times otherwise necessary to allow lightly damped airbag oscillations to die away. The airbag was inflated a small distance above the impact target (to ensure no contact during inflation) and then accelerated under Mars gravity to strike the ground or rock with the required initial velocity conditions. During impact, the resultant acceleration at the payload centre of mass node was monitored for triggering the vents. A crude filtering was employed to avoid premature triggering due to signal noise by defining a cumulative time above the 65g threshold before the vents were 'opened' **(Figure 5)**. Some experimentation was necessary to achieve consistent triggering.

Figure 5: Typical Acceleration Response and Vent Trigger Event (enlarged area)

The Wang-Nefske airbag model within LS-DYNA was used to simulate the thermodynamic behaviour of the gas. Nitrogen was considered in this study. The vents themselves were not physically modelled, instead the mass flow rate through the open vents was calculated for each time step assuming adiabatic flow through an orifice using the relationship:

$$\dot{m} = k \cdot A \cdot \frac{p}{\sqrt{RT}} \cdot Q^{1/\gamma} \cdot \sqrt{\frac{2\gamma}{(\gamma - 1)} \cdot \left[1 - Q^{(\gamma-1)/\gamma}\right]}$$

$$Q = \frac{p_e}{p} \qquad \text{if} \quad Q > Q_{crit}$$

$$Q = Q_{crit} = \left(\frac{2}{\gamma + 1}\right)^{\gamma/(\gamma - 1)} \quad \text{if } Q < Q_{crit}$$

where,

k = discharge coefficient
A = vent area
R = gas constant
p = airbag pressure
p_e = external atmospheric pressure
T = temperature
γ = ratio of specific heats

The modelling approach ignores the finite opening time of the vent and any changes in its shape during the impact (the orifice is either closed or completely open with a constant area). Because of the low ambient pressure on Mars, the pressure ratio Q is less than the critical value (Q_{crit} = 0.53) for almost all of the venting duration, resulting

in choked sonic flow conditions. (This is not the case if the airbag is inflated to the equivalent gauge pressure and vented to ambient pressure on Earth: in this case the initial flow is subsonic. Hence, a large vacuum chamber is necessary to correctly simulate venting in tests).

The assumption of adiabatic flow is a reasonable one because of the short impact event duration and limited heat exchange to the surrounding atmosphere. For the initial inflation step, however, steady state gas conditions were required with a specified pressure. In reality, the airbag is inflated during the parachute descent some time before impact and regulated to attain a preset pressure at the prevailing ambient atmospheric temperature. Within the FE analysis, it was necessary to inflate the airbag isothermally to achieve this and then switch to the adiabatic assumption for venting in the automated solution sequence. This differs from typical automotive airbag conditions where both inflation and venting are assumed to occur adiabatically. It was necessary to use a modified version of the LS-DYNA code **[4]** to permit the switching of the thermodynamic assumptions within a single analysis run.

Parameter	Value
Rover/Platform Payload	
Mass	385 kg
CoM	(0, 0, 125) mm
Inertia I_{XX}	60 kg.m^2
Inertia I_{YY}	70 kg.m^2
Inertia I_{ZZ}	120 kg.m^2
Platform Diameter	∅1.9 m
Platfrom Thickness	75 mm
Airbag	
Gas	N_2
Topology	6 vented sector compartments + un-vented toroid
Geometry	Patched semi-elliptical profiles, see **Figure 10**
Toroid Inflation Pressure	200 kPa
Height	3.0 m to 5.0 m
Diameter	0.8 m to 1.2 m
Compartment Inflation Pressure	15 kPa to 55 kPa
Vent Area	0.15 m^2 to 0.40 m^2
Vent Discharge Coefficient	0.7
Vent Control	All compartments vented at 65 g CoM acceleration threshold
Airbag Fabric	
Material	350 gsm Silicone-Coated 1500 denier HT Vectran
Thickness	0.32 mm
Youngs Modulus	15.2 GPa
Shear Modulus	0.7 GPa
Tensile Strength	170 N/mm
Mars Environment	
Gravity	0.38 g
Temperature	-89 °C
Atmospheric Pressure	440 Pa
Surface Friction Coefficient	0.9

Table 1: FEM Parameters. Design Variables for Optimization are Highlighted

6.0 Surrogate Model Building

The success of the surrogate response modelling approach depends on the quality of the response surface approximations. These must reproduce highly non-linear response functions over a large parameter space from only a limited number of analysed points. The quality of the response surface approximations are determined by:

1) Selection of the sampling points in the parameter space - Design of Experiments (DoE)

2) Selection of the surface-fitting algorithm through the sample points.

6.1 Design of Experiments

The DoE method adopted was based on a Uniform Latin Hypercube with the addition of the corner points in the parameter space, termed an Extended Uniform Latin Hypercube (EULH). This ensures extreme parameter combinations are included in the analysed set and gives a uniform filling of the design space.

The Uniform Latin Hypercube (ULH) method divides each of the N parameters into P levels, where P is the number of 'test points' required, assigns a single point to each level and then seeks an optimum distribution of points that uniformly fills the parameter space. The physical analogy of the optimum distribution is the minimisation of the total potential energy of the P particles with mutually repulsive forces inversely proportional to the square of the distances between them. In the EULH method, the 2^N corner points of the parameter space are first assigned and then the remaining ($P - 2^N$) points are determined with the same objective of uniform space-filling **(Figure 6)**.

For airbag design optimization, 4 variables were considered (N=4) and 40 combinations of these parameters (P=40) were sought as the test points for the FE analysis runs. The $2^4 = 16$ corner points were specified by the parameter range extremes and the remaining (40 – 16) = 24 points were determined using a permutation genetic algorithm[5] built into HyperStudy to give the required optimum filling of the 4-dimensional parameter space.

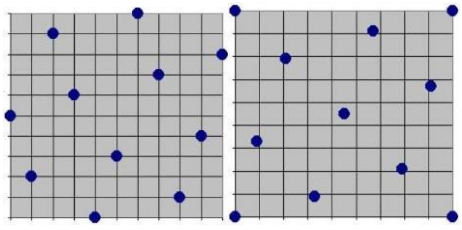

Figure 6: Left: Uniform Latin Hypercube (ULH). Right: Extended Uniform Latin Hypercube (EULH). For N=2, P=11 Parameter Space

6.2 Response Surface Fitting

The response surface-fitting algorithm used was the Moving Least Squares Method (MLSM) **[6] [7]** built in to HyperStudy.

The MLSM is a generalisation of a classical weighted least squares curve-fitting method where the 'weights' are not constant, but are functions of the Euclidean distance from the surrogate model evaluation point to a specific sampling point in the design space. The weighting function decays with distance so that nearby sampled points have a greater influence on the form of the approximated surface than those some distance away. A 'closeness of fit' parameter permits the user to adjust the weighting decay function, effectively the radius of influence beyond which the weighting factor approaches zero. Setting the 'closeness of fit' parameter to a large value results in an approximated surface with a tight fit to the sample points, but which is then susceptible to numerical noise in the sampled data. Reducing the 'closeness of fit' parameter eliminates the effects of noise by giving a more 'averaged' approximation over the parameter space. By adjusting the 'closeness of fit' parameter it is possible to get good approximations to highly non-linear response functions without the distorting effects caused by noise.

In the case of the airbag analysis, the peak deceleration experienced by the payload during impact yielded a response function which was both non-smooth and 'noisy' with respect to both design and external variables. The airbag trigger threshold was set at 65g and the maximum acceptable level was limited to 80g. Decelerations in this interval were acceptable. However, inadequate designs or extreme landing conditions could cause the airbag to 'bottom-out' with the payload platform making hard contact with a rock or the ground. This resulted in extreme value spikes, sometimes in excess of 1000g in the resulting deceleration response. This type of response surface is analogous to Rosenbrock's 'banana valley function' with random noise **(Figure 7)** in which a smooth, relatively flat valley containing the points of interest is surrounded by steep-edge 'cliffs' with spikes superimposed on the high plateau. To approximate the peak deceleration response function, the high noise area was first capped to a level of 1000 m/s^2 (~100g) and an MLSM fit was made to the capped response data.

The quality of the MLSM in approximating this type of response compared to a traditional Least Squares approximation is evident in the example of the capped banana valley function **(Figure 8)**. The Least Squares method assigns equal weight to all points so smoothes out the steep valley sides, blurring the true shape. By contrast, the MLSM retains the essential form of the function.

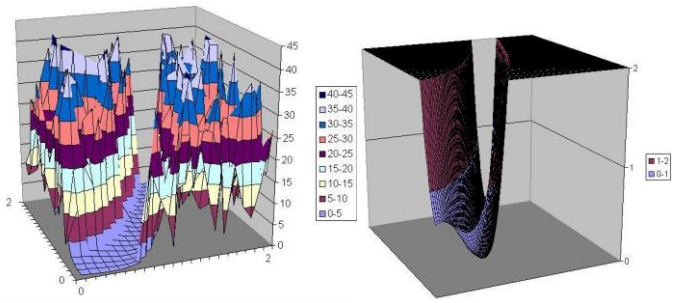

Figure 7: Left: Rosenbrock's Banana Valley Function with Random Noise. Right: Capped Function

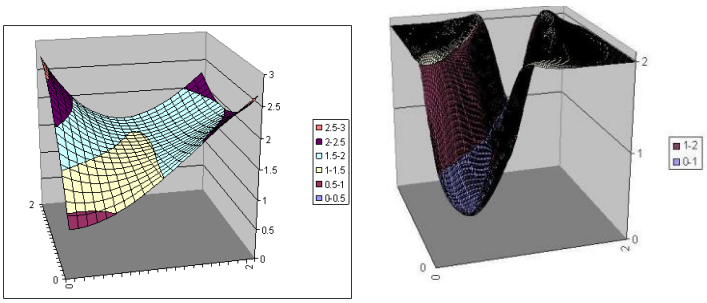

Figure 8: Left: Least Squares Approximation to Capped Banana Valley Function. Right: MLSM Approximation, Showing Improved Conformance

7.0 Design Optimization Problem

7.1 Problem Formulation

The airbag design optimization problem was initially set up as follows:

Minimise the overall airbag system mass, defined by the objective function:

$M_A = M_F + M_G + M_{GS} + M_O$

where,

M_A = total airbag system mass
M_F = fabric mass = $1.20\gamma A_F$
M_G = gas mass = $1.05/RT.(p_1V_1+p_2V_2)$
M_{GS} = gas storage system mass
= $1.52M_G + 0.75kg$
M_O = vents, pipework, valves, packing cover mass
= $0.06M_F + 2.0kg$

γ = fabric mass / area (kg/m^2)
A_F = total unstressed fabric area (m^2)
1.20 = seams / reinforcement factor
R = gas constant (J/kgK)
T = inflation (ambient) temperature (K)
p_1 = main compartment inflation pressure (N/m^2)
V_1 = total inflated vol. of main compartments (m^3)
p_2 = toroid inflation pressure (N/m^2)
V_2 = inflated vol. of toroid (m^3)
1.05 = gas overfill factor

Subject to the response constraints **(Table 2)**:

Constraint Parameter	Upper Limit
Peak Acceleration a_{max}	80 g
Max Fabric Stress σ_{VMmax}	533 MPa
Final Attitude θ_{final}	$\pm$ 60°
Residual Energy E_{resid}	15000 J

Table 2: Response Function Constraints For Optimization

For the following design impact cases **(Table 3)**:

Landing Condition Parameter	Case 1 Vertical	Case 2 Lateral
Vertical Velocity V_V	25 m/s	25 m/s
Lateral Velocity V_H	0 m/s	16.3 m/s
Pitch Attitude θ_0	0°	20°
Pitch Rate Ω	0 deg/s	0 deg/s
Ground Slope	0°	10°
Terrain	Flat	500mm rock

Table 3: Design Landing Cases for Optimization

By varying the following design parameters over the indicated ranges **(Table 4)**:

Design Parameter	Lower Limit	Upper Limit
Airbag Diameter D	3.0 m	5.0 m
Airbag Height H	0.8 m	1.2 m
Inflation Pressure p	15 kPa	55 kPa
Vent Area A /each	0.15 m^2	0.40 m^2

Table 4: Design Variable Limits for Optimization

And fixing all other variables as per **Table 1**.

The airbag system mass objective function (M_A) takes into account the mass of the fabric, the inflation gas, the gas storage system and other items. A high pressure gas storage system is assumed (rather than a gas generator), consistent with the use of nitrogen gas. The parametric relationship for the storage system mass is based on carbon-fibre over-wrapped aluminium gas bottles with a storage pressure of 200-300 bar.

The response constraints in **Table 2** relate to potential landing failure modes. The peak acceleration (a_{max}) is the maximum resultant acceleration at the payload centre of mass. The limit of 80g is dictated by the capabilities of the rover payload and support structures.

The maximum permitted stress level (σ_{VMmax}) is based on the fabric tensile strength taking into account an 85% knock-down for variability and degradation due to heat sterilisation. This is compared with the highest recovered Von Mises membrane stress in all airbag finite elements except those immediately adjacent to joints. These areas are reinforced by seams and additional local layers, which were not included in the FE model.

The maximum permitted final attitude angle (θ_{final}) is set as a failure condition for roll-over. θ is the pitch attitude angle of the normal to the platform with respect to the gravity vector, with 0° vertically upwards. The lack of protection around the upper part of the rover payload means that an 'upside down' landing, i.e. θ_{final} ~ 180°, will result in structural damage and prevent rover egress from the platform (it has no self-righting capability). In effect, the angular inversion criterion is covered by the maximum acceleration requirement (a_{max}) since a soft upside down landing is extremely unlikely. However, several seconds of elapsed time must be analysed to determine whether the lander comes to rest inverted or strikes the ground hard in this attitude. The same problem also exists for landings with excessive bounce where the analysis must run for a long time to cover a secondary impact onto the anti-bottoming toroid, or subsequent inversion. These analysis times are impractical, particularly for a large number

of runs, and differ greatly for different airbag designs or landing conditions. The inversion and excessive bounce failure criteria were therefore re-cast in terms of a lower final pitch angle (θ_{final}) and residual energy (E_{resid} = total kinetic plus potential energy) after a fixed analysis time of 200ms. This was sufficiently long to capture the primary impact event and some of the subsequent rebound behaviour. The threshold criteria of $E_{resid} \leq 15000$ J and $\theta_{final} \leq 60°$ were by necessity fairly arbitrary and largely a matter of judgement. The residual energy threshold corresponds to about 8% of the initial impact kinetic energy and is within the maximum stroke capability of the anti-bottoming toroid. The pitch angle limit screens out failure cases where the energy criterion is met but there is still sufficient energy in some circumstances to cause the lander to invert (only about 1500 J is sufficient to rebound the lander to an 'edge-on' stability limit from where it could tip over).

The two design cases summarised in **Table 3** and depicted in **Figure 9** were selected to constrain the airbag design for landing condition extremes. In Case 1, with a vertical impact, the contact area with the ground is maximised, maximising the force and therefore platform deceleration. This case pushes the design towards small airbag diameters or lower pressures, but with a relatively tall profile to give the required stroke. In Case 2, a high lateral landing velocity component, pitch-down angle, up-slope landing site and a large rock are added. This case was selected to invoke 'roll-over' (inversion) or 'dive-through' (platform edge contact on the rock). This case tends to push the airbag design towards a larger plan area and higher pressure. Hence, the optimum is forced to compromise the design variables between the conflicting requirements of the two extremes.

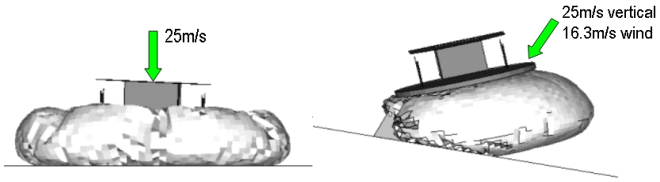

Figure 9: Landing Cases for Optimization. Left: Case 1, Vertical Impact on Flat Ground. Right: Case 2, with Additional Wind Velocity, Pitch Attitude, Landing Site Scope and Rock

The design optimization was limited to the 4 main design variables listed in **Table 4**. All other parameters were fixed with the values given in **Table 1**. The airbag main envelope geometry was constrained to the profile shown in **Figure 10**, which consists of blended semi-elliptical curves all scaled to two primary geometric variables: diameter (D) and height (H). The cross-sectional shape was revolved through 360° to generate the complete (unstressed) envelope geometry. The 'morphing' capability within HyperMesh[8] was used to automatically generate FE models for all combinations of D and H from the DoE by retaining the baseline FEM element connectivity and distorting the element mesh accordingly. The toroidal anti-bottoming compartment was unchanged.

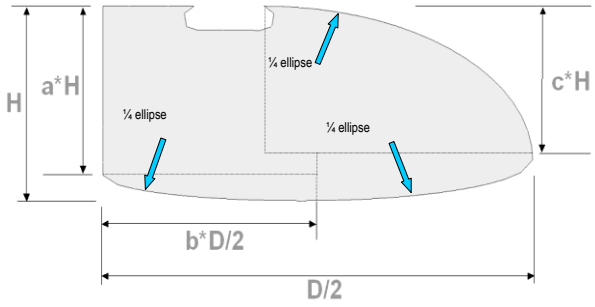

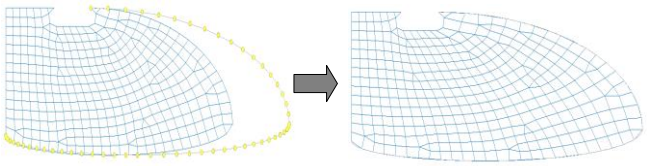

Figure 10: Airbag Geometry for Optimization. Top: Semi-elliptical Profile Related to Primary Geometry Variables D and H. Bottom: Automated Morphing of FE Model Mesh

The inflation pressure (p) and vent area (A) were single value parameters easily changed within the FE model deck for the DoE runs.

The upper and lower bounds on all the free design variables for limiting the design parameter space were based on judgement. The relatively large range on inflation pressure was necessary to cover the corresponding range in the airbag volume at the geometric extremes.

7.2 Optimization Analysis

40 FE analysis runs were performed for each landing case (i.e. a total of 80 runs) for the design parameter combinations determined from the EULH DoE. Set-up of the FE models and management of the analysis runs was performed using HyperStudy, with the LS-DYNA simulations run in parallel in batches of 16 on a Linux Cluster (Intel Xeon 2.8GHz processor). The typical run time for a 200ms simulation was 10.5 CPU hours and total analysis time was ~ 50 hours.

The response parameters listed in **Table 2** were extracted from the FE analyses. For decelerations, high responses (hard contacts) where capped at 1000 m/s^2 (~ 100g) to suppress noise in the 'failed region' of the response surface. Surrogate response surfaces were fitted to the analysis results using the MLSM, described above. These showed that the size of the 'sweet spot' – the design space that fulfilled all the constraint requirements – was small. Furthermore, the objective function based on airbag system mass showed little variability across this region. Therefore, the objective was revised from a minimisation of mass to the minimisation of residual energy, on the basis that this would yield a design with the most potential of maximising the probability of a successful landing under a wider range of landing conditions.

Further FE runs were performed for combinations of design parameters within the 'sweet spot' region to confirm the surrogate model predictions and to improve the fidelity of the response functions in the constrained space. From this exercise, the 'optimum design' parameters listed in **Table 5** were selected. Significantly, the vent area is at the upper limit of the originally prescribed range, suggesting that this may have been too constraining and that larger vent areas may be beneficial in future studies.

Design Parameter	Optimum
Airbag Diameter D	4.41 m
Airbag Height H	1.00 m
Inflation Pressure p	30.3 kPa
Vent Area A /each	0.40 m^2
System Mass M_A	18 kg

Table 5: Optimised Airbag Design Parameters

The optimised airbag design was carried through to the probabilistic assessment.

8.0 Probabilistic Assessment

The objective of the robustness assessment was to answer questions (2) and (3) of the study objectives – to determine the probability of a successful landing of the optimised airbag design and to investigate how sensitive this was to changes in the targeted landing site or parachute performance.

8.1 Problem Formulation

For a preliminary assessment of reliability, 4 landing condition parameters: wind velocity, rock size, pitch attitude and pitch rate were selected as the most important external factors determining landing success or failure. The calculation of landing success probability requires the success/failure constraint parameters listed in **Table 2** to be evaluated for a large number of permutations of the landing condition variables based on their own relative occurrence probabilities. This Monte Carlo analysis was performed using surrogate models of the response surfaces generated in the same way as the optimization procedure **(**Error! Reference source not found.**)**. 80 FE analysis runs were performed corresponding to combinations of the landing parameters derived from the EULH DoE. To permit batch processing of these runs it was necessary to automate the set-up of the FE models to vary rock geometry and apply the initial conditions for impact **(Figure 11)**. Here it was necessary to consider negative as well as positive pitch angles and rates. The lander was always orientated to contact the single rock at the lower leading edge in the plane of motion. The rock geometry was based on the truncated tetrahedron shape shown in **Figure 11** with a height equal to half the diameter. The initial airbag contact point was at an upper corner.

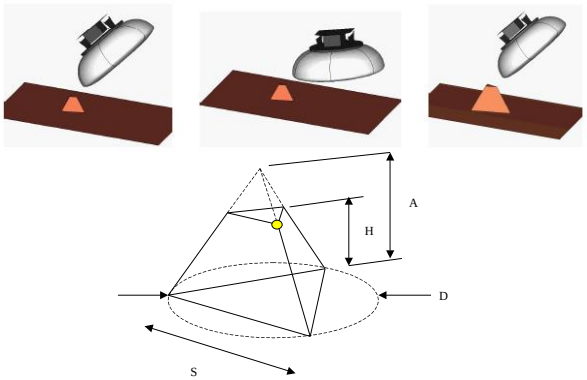

Figure 11: FEM boundary Conditions for Reliability Assessment DoE runs. Top: Lander Attitude and Rock Position. Bottom: Rock Geometry

As with the optimization problem, the LS-DYNA simulation runs were run in parallel in batches managed using HyperStudy. Surrogate response models for the success/failure constraint parameters listed in **Table 2** were fitted to the results using the MLSM (with the same 100g capping of acceleration responses).

8.2 Baseline Reliability

Once the surrogate response model was generated it was relatively simple to perform a Monte Carlo analysis using probability density functions (PDFs) of the 4 landing condition variables as summarized in **Table 6**.

Parameter	PDF

Wind Velocity V_H	Weibull $\alpha = 2$	β = 7.97 m/s
Rock Height h	Exponential	β = 0.196m
Pitch Angle θ_0	Gaussian	$3\sigma = 30°$
Pitch Rate Ω_0	Gaussian	$3\sigma = 20°/s$

Table 6: Landing Parameter PDFs for Baseline Reliability Assessment

Wind velocity data were derived from the European Mars Climate Database (EMCD v3.0) **[9]**. This 3D global circulation model for the Mars atmosphere gives data on a 5° longitude x 5° latitude grid at 32 heights for 2 hour intervals during the Martian day averaged for each of the 12 'seasons'. For the baseline ExoMars mission, the wind velocity data were derived for the 45°N to 45°S central latitude band for landing during Season 12 and assumed the Mars Global Surveyor dust-loading scenario **(Figure 12)**. A Rayleigh PDF gave the best fit to the model data. This is a special case of a 2-parameter Weibull distribution with α = 2, frequently used in terrestrial windspeed probability models. The PDF was matched to the EMCD model mean resultant wind velocity of 7.97 m/s, but had a slightly higher standard deviation of 3.69 m/s (compared to 3.45 m/s from the EMCD data). The PDF is given by:

$$f(x) = \frac{2}{\beta^{\alpha}} \cdot x \cdot \exp\left[-\left(x/\beta\right)^2\right]$$

$$\mu = \frac{\sqrt{\pi}}{2} \cdot \beta$$

$$\sigma^2 = \left(1 - \frac{\pi}{4}\right) \cdot \beta^2$$

where,

x = wind velocity
μ = mean
σ = standard distribution
α = 2

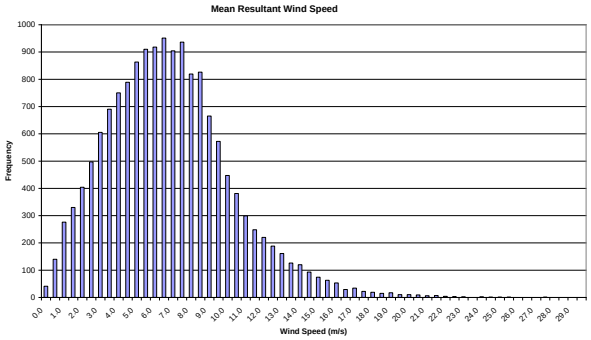

Figure 12: Baseline Windspeed PDF (EMCD season 12, 45°N to 45°S, MGS dust loading scenario)

The rock size distribution was based on the exponential PDF model proposed by Golombek et al[10] as a function of general rock abundance **(Figure 13)**. This fits the probability distribution model parameters to observed rock sizes at the Viking and Mars Pathfinder landing sites on Mars. The PDF is given by:

$$f(h) = \frac{1}{\beta} \exp^{=\frac{h}{\beta}} \quad for\ h > 0$$

where,

$$\beta = \frac{1}{\left[3.58 + \frac{0.304}{k}\right]}$$

h = rock height
k = overall rock abundance fraction

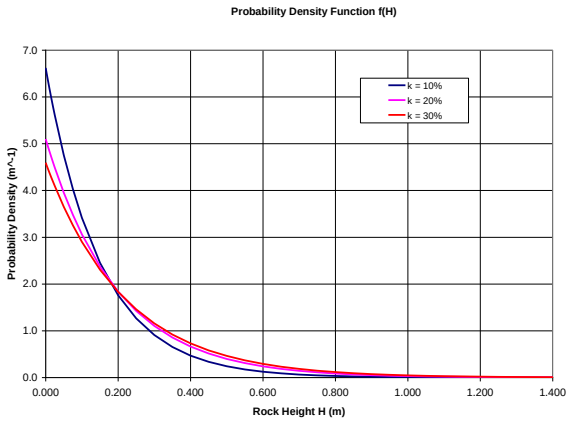

Figure 13: Rock Height PDFs for Different Overall Rock Abundances (rock height = ½ rock diameter)

For the ExoMars mission, a baseline worst-case landing site with an overall rock abundance (i.e. fractional area covered in rocks) of k = 20% was considered. Rock heights were assumed to be half the rock diameter. This resulted in an exponential PDF with a mean rock height of 0.196 m and standard deviation of 0.196 m.

The pitch attitude angle and rate at impact are random variables due to motion whilst suspended underneath the main parachute. These were idealised as Gaussian normal distributions with zero means and 3-sigma levels set to $\pm$ 30° and $\pm$ 20°/s respectively.

Monte Carlo simulations were performed using the landing parameter PDFs and surrogate response models. **Figure 14** shows a typical 'anthill plot' of landing condition sample points derived from the PDFs.

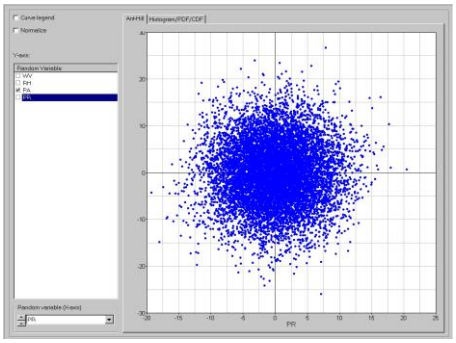

Figure 14: Anthill Plot for Pitch Angle and Pitch Rate for 10,000 point Monte Carlo Analysis

Responses exceeding the criteria of **Table 2** were deemed failures and tallied up to determine an overall failure probability. The reliability was given by the probability of success = 1 – P(failure). Samples of 100, 1,000 and 10,000 points were run to ascertain the size for convergence **(Table 7)**. Because the Monte Carlo runs operated on the surrogate response model, there was little computational cost of large samples. Good convergence was achieved for 10,000 points, taking only about 5 minutes to run on a desktop PC.

Sample Size	Success Probability
100	67.0%
1000	68.3%
10000	68.6%

Table 7: Convergence of Predicted Landing Success Probability with Monte Carlo Sample Size

The success probabilities calculated for each response criterion are broken down in **Table 8**. (Note that the total failure probability is less than the sum of the individual criteria because more than one may cause failure in some cases). The overall reliability is low at only 67%, indicating insufficient robustness in the design for the range of landing conditions considered. The angular attitude criterion (θ_{final}) is the primary contributor to this poor performance, indicating 'roll-over' as a dominant failure mode. An investigation of the parameters where this failure mode was active and FE analysis runs with similar conditions suggested that initial trailing edge contact was a particular problem **(Figure 15)**. This caused over-turning moments which the simple simultaneous all-vent control strategy couldn't always effectively counter. This also reflects the fact that this landing attitude was not considered as a case in the original design optimization.

Criterion	Success Probability
Peak Acceleration a_{max}	87.6%
Max Fabric Stress σ_{VMmax}	99.8%
Final Attitude θ_{final}	77.4%
Residual Energy E_{resid}	90.7%
Overall	**68.6%**

Table 8: Baseline Reliability. Landing Success Probability and Breakdown for each Criterion

Figure 15: Roll-over Failure Mode for Trailing Edge Contact Landing Attitudes

8.3 Reliability Sensitivity to Relaxed Landing Conditions

The surrogate response model made it relatively simple to investigate the effect of relaxed landing conditions on the success probability. Three changes were considered:

1) Morning landing only (between 00:00 and 12:00 Mars LST) in a reduced latitude band of 45°N to 10°S
2) Landing at sites restricted to a maximum rock coverage of 10%
3) Reducing 3σ pitch angles and rates due to improved parachute design or reduced uncertainty.

The objective of the morning landing constraint was to reduce windspeeds (on the basis the atmosphere becomes more disturbed as it is heated during the day). The EMCD model however yielded only a modest reduction in mean windspeed of about 0.5m/s (**Table 6** compared to **Table 9**). The targeting of landing sites with a reduced overall rock coverage modified the rock height PDF to that given in Table 9 and shown in **Figure 13**).

Parameter	PDF	
Wind Velocity V_H	Weibull α = 2	β = 7.49 m/s
Rock Height h	Exponential	β = 0.151m
Pitch Angle θ_0	Gaussian	3σ = 20°
Pitch Rate Ω_0	Gaussian	3σ = 15°/s

Table 9: Landing Parameter PDFs for Reliability Sensitivity Assessment

The resulting improvements in overall landing reliability due to the relaxed PDFs are summarised in **Table 10** in the cumulative order they are applied. The effect of the relatively small relaxation in the windspeed distribution is minor, as too is the effect of less rocky terrain, which in this case reflects the general insensitivity to rock size. However, there is a significant improvement in reliability of 10% due to reduced variability in the pitch angle and rate at landing.

PDF Changed	Success Probability
Baseline	68.6%
Wind Velocity	70.7%
Rock height	70.8%
Pitch Angle & Rate	80.8%

Table 10: Sensitivity of Overall Landing Reliability to Changes in Landing Parameter PDFs

The reliability breakdown of the various failure modes for the cumulative effect of all the modified PDFs is summarised in **Table 11**. The peak acceleration ('dive-through') and final attitude ('roll over') criteria now both yield

similar success contributions of about 90%. The overall reliability is improved to ~81%, but is still some way short of a target >95%.

Criterion	Success Probability
Peak Acceleration a_{max}	88.5%
Max Fabric Stress σ_{VMmax}	99.9%
Final Attitude θ_{final}	89.4%
Residual Energy E_{resid}	95.5%
Overall	**80.8%**

Table 11: Landing Success Probability for the Cumulative Effect of Relaxed Landing Condition PDFs

9.0 Conclusions

A methodology was successfully developed for the application of surrogate response modelling techniques to the analysis of vented airbags. This was found to be a valuable tool that can be applied both to design optimization and the assessment of robustness under a wide range of landing conditions. The ability to perform 10,000 point Monte Carlo simulations from a limited set of FE analysis runs was found to be particularly powerful, giving insight into landing scenarios that cause specific modes of failure as well as the determination of an overall reliability figure. Such a capability is invaluable in this application where fully representative ground testing is difficult and expensive.

The vented airbag for ExoMars, with a simple simultaneous all-vent control strategy was found to have insufficient reliability. The landing success probability was estimated to be between 69 to 81%, depending on the range of landing conditions considered. Optimization of the design indicated that larger vents may offer performance improvements (these were at the originally prescribed upper bound), but it is likely that the necessary improvement in reliability can only be attained with more complex control algorithms in which the compartment vents are triggered at different times. Such strategies should aim to counter over-turning moments and differentiate between pitch-up and pitch-down landing attitudes.

In the future, it is recommended that pitch-up as well as pitch-down cases are considered for optimization of the design. Also, longer FE analysis simulation times are suggested to remove some of the uncertainty associated with setting the residual energy and final pitch angle failure criteria for roll-over or excessive bounce.

9.0 References

[1] **'Improved Inflatable Landing Systems for Low Cost Planetary Landers.'** Northey, D and Morgan, C. 5th IAA International Conference on Low-Cost Planetary Missions. Acta Astronautica October 2005.

[2] **'Impact Analyses and Tests of an Airbag Landing System for Small and Medium Sized Probes. Proc. Conference on Spacecraft Structures, Materials & Mechanical Testing'** Schweickert, G., Scheulen, D and Hass, G, Noordwijk, The Netherlands, March 27-29 1996. (ESA SP-386, June 1996).

[3] **Altair HyperStudy 7.0 SP1** (2005). Altair Engineering Inc.

[4] **LS-DYNA Version 971_4607** (2005). Livermore Software Technologies Corporation, Special build by Art Shapiro, LSTC Technical Support, used with thanks.

[5] **'Formulation of the Optimal Latin Hypercube Design of Experiments using a Permutation Genetic Algorithm.'** Bates, S.J., Sienz, J. and Toropov, V.V. Paper AIAA-2004-2011, 45th AIAA/ASME/ASCE/AHS/ ASC Structures, Structural Dynamics, and Materials Conference. Palm Springs, CA, April 19-22 2004.

[6] **'Moving Least Squares Method for Reliability-Based Design Optimization.'** Choi, K. K. Youn, B., and Yang, R-J. 4th World Congress of Structural and Multidisciplinary Optimization, Dalian, China, June 4-8 2001.

[7] **'Design Optimization and Stochastic Analysis based on the Moving Least Squares Method.'** Toropov, V.V., Schramm, U., Sahai, A., Jones, R. and Zeguer, T, Paper 9412, 6th World Congress of Structural and Multidisciplinary Optimization, Rio de Janeiro, Brazil, May 2005.

[8] **Altair HyperMesh 7.0** (2005) (incorporating HyperMorph), Altair Engineering Inc.

[9] **European Mars Climate Database** (EMCD) v3.0. www-mars.lmd.jussieu.fr.

[10] **'Probability of Impacting and Accessing Rocks at the MER Landing Sites.'** Golombek, M.P., Haldemann, A., DiMaggio, E., Schroeder, R. and Matijevic, J. 4th MER Landing Site Workshop, Arcadia, USA, Jan 8-10 2003.

